Article

Theoretical Study on the Photolysis Mechanism of 2,3-Diazabicyclo[2.2.2]oct-2-ene

Hui Chen, and Shuhua Li

J. Am. Chem. Soc., **2005**, 127 (38), 13190-13199• DOI: 10.1021/ja050002p • Publication Date (Web): 01 September 2005

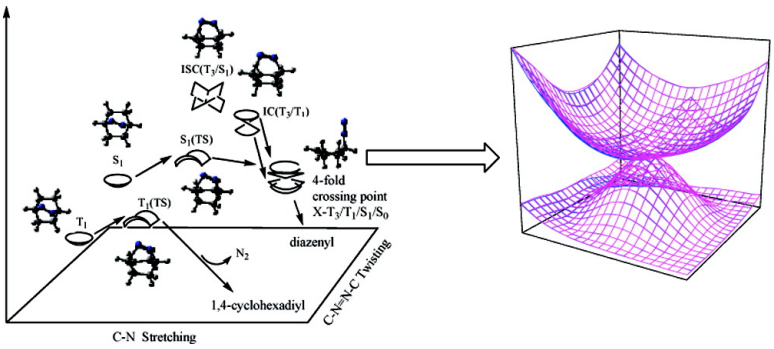

More About This Article

Additional resources and features associated with this article are available within the HTML version:

- Supporting Information
- Access to high resolution figures
- Links to articles and content related to this article
- Copyright permission to reproduce figures and/or text from this article

View the Full Text HTML

J|A|C|S
ARTICLES
Published on Web 09/01/2005

Theoretical Study on the Photolysis Mechanism of 2,3-Diazabicyclo[2.2.2]oct-2-ene

Hui Chen and Shuhua Li*

Contribution from the Lab of Mesoscopic Chemistry, Institute of Theoretical and Computational Chemistry, Department of Chemistry, Nanjing University, Nanjing 210093, People's Republic of China

Received January 1, 2005; E-mail: shuhua@nju.edu.cn

Abstract: A CASPT2/CASSCF study has been carried out to investigate the mechanism of the photolysis of 2,3-diazabicyclo[2.2.2]oct-2-ene (DBO) under direct and triplet-sensitized irradiation. By exploring the detailed potential energy surfaces including intermediates, transition states, conical intersections, and singlet/triplet crossing points, for the first excited singlet (S_1) and the low-lying triplet states (T_1, T_2, and T_3), we provide satisfactory explanations of many experimental findings associated with the photophysical and photochemical processes of DBO. A key finding of this work is the existence of a significantly twisted S_1 minimum, which can satisfactorily explain the envelope of the broad emission band of DBO. It is demonstrated that the S_1 ($n-\pi^*$) intermediate can decay to the T_1 ($n-\pi^*$) state by undergoing intersystem crossing (rather inefficient) to the T_2 ($\pi-\pi^*$) state followed by internal conversion to the T_1 state. The high fluorescence yield and the extraordinarily long lifetime of the singlet excited DBO are due to the presence of relatively high barriers, both for intersystem crossing and for C−N cleavage. The short lifetime of the triplet DBO is caused by fast radiationless decay to the ground state.

1. Introduction

Azoalkanes have attracted much attention due to their ability to form radicals by thermal and photochemical denitrogenation.[1−8] The denitrogenation of azoalkanes has become a viable route for structurally unusual compounds in organic synthesis. However, the quantum yields for the photochemical extrusion of nitrogen depend strongly on the structure of the azoalkane, varying from as high as unity to essentially zero. For example, azoalkanes containing the bicyclo[2.2.1] moiety photoeliminate nitrogen efficiently, while azoalkanes with the bicyclo[2.2.2] moiety are "reluctant" azoalkanes which have a low efficiency for deazotation, both thermally[9] and photochemically.[13−15] As representative examples of these two cases, 2,3-diazabicyclo-[2.2.1]hep-2-ene (DBH)[10,23,29−30] and 2,3-diazabicyclo[2.2.2]oct-2-ene (DBO)[11−22,24] have been extensively studied for exploring the photolysis mechanism, respectively. In Scheme 1, we have collected known experimental information on the excited states, intermediates, and products involved in the photolysis of DBO.

Scheme 1

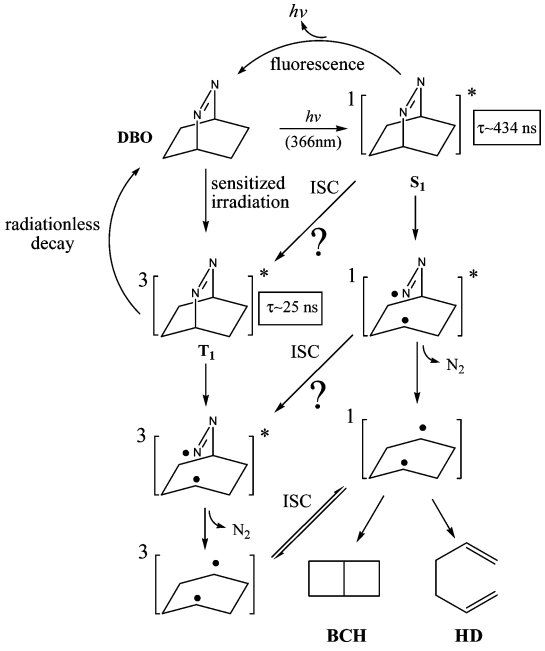

Steel and co-workers first reported extensive photophysical and photochemical measurements on DBO and DBH.[13,14] They found that the absorption spectra of both compounds are highly structured. For DBO, the absorption peak at 26610 cm^{-1} (76.1 kcal/mol) was assigned to the 0−0 transition. The emission

(1) Engel, P. S. *Chem. Rev.* **1980**, *80*, 99.
(2) Rau, H. *Angew. Chem., Int. Ed. Engl.* **1973**, *12*, 224.
(3) Meier, H.; Zeller, K. P. *Angew. Chem., Int. Ed. Engl.* **1977**, *16*, 835.
(4) Adam, W.; Nau, De Lucchi, O. *Angew. Chem., Int. Ed. Engl.* **1980**, *19*, 762.
(5) Adam, W.; Grabowski, S.; Wilson, R. M. *Acc. Chem. Res.* **1990**, *23*, 165.
(6) Dougherty, D. A. *Acc. Chem. Res.* **1991**, *24*, 88.
(7) Engel, P. S.; Hayes, R. A.; Kiefer, L.; Szilagyi, S.; Timberlake, J. W. *J. Am. Chem. Soc.* **1978**, *100*, 1876.
(8) Cohen, S. G.; Zand, R.; Steel, C. *J. Am. Chem. Soc.* **1961**, *83*, 2895.
(9) Thermal deazotation of DBO: (a) Cohen, S. G.; Zand, R. *J. Am. Chem. Soc.* **1962**, *84*, 586. (b) Allred, E. L.; Hinshaw, J. C. *J. Chem. Soc., Chem. Commun.* **1969**, 1021. (c) Snyder, J. P.; Harpp, D. N. *J. Am. Chem. Soc.* **1976**, *98*, 7821. (d) Martin, H. D.; Heiser, B.; Kunze, M. *Angew. Chem., Int. Ed. Engl.* **1978**, *17*, 696. (e) Engel, P. S.; Allgren, R. L.; Woo-Ki Chae; Leckonby, R. A.; Marron, N. A. *J. Org. Chem.* **1979**, *44*, 4233. (f) Engel, P. S.; Nalepa, C. J.; Horsey, D. W.; Keys, D. E.; Grow, R. T. *J. Am. Chem. Soc.* **1983**, *105*, 7102.

10.1021/ja050002p CCC: $30.25

spectrum of DBO is characterized by a broad band with a maximum at about 23000 cm^{-1} (65.8 kcal/mol), which is absent from the highly structured emission spectrum of DBH. Fluorescence quantum yields of DBO were found to be 0.56 ± 0.10 in the gas phase and 0.37 in acetonitrile. No phosphorescence was detected for DBO under any conditions. These experiments[14] also showed that on direct irradiation in the gas phase deazotation occurs with a high quantum yield (0.50), but exclusively from the triplet excited state of DBO, while on sensitization the deazotation yield depends strongly on the energy of the chosen triplet sensitizer. The deazotation yield is much higher with benzene (E_T = 84.7 kcal/mol) than with biacetyl (E_T = 54.9 kcal/mol) as a sensitizer.[14]

Since the work of Steel et al. many experimental studies on the photolysis of DBO and its derivatives have appeared.[15−22] Engel et al. have studied the effect of fused rings and bridgehead substituents on the photochemical and photophysical properties of DBO in different solvents.[15] For DBO in benzene, they found deazotation quantum yields of $\Phi_r = 0.018$ on direct irradiation (366 nm) and $\Phi_r = 0.014$ on triplet-sensitized irradiation (313 nm). The fluorescence quantum yield $\Phi_f = 0.39$ and the lifetime of the singlet excited state (434 ns) were also measured. Clearly, the lifetime of the S_1 state of DBO is much longer than that of the corresponding singlet excited state of DBH[23] (2 ns). The activation energies for deazotation by direct and triplet-sensitized irradiation were estimated to be 8.6 and 9.0 kcal/mol, respectively.

By time-resolved photoacoustic calorimetry, Caldwell et al. determined that in cyclohexane the triplet state of DBO lies at 51.9 ± 0.6 kcal/mol and that its lifetime is 25 ns.[21] The short lifetime of the triplet state, the absence of phosphorescence, and the low quantum yield for deazotation suggest fast radiationless decay from the T_1 state of DBO.

The distribution of products (bicyclo[2.2.0]-hexane (BCH) and 1,5-hexadiene (HD)) from the photolysis of DBO is well documented.[15,19] Direct irradiation of the N=N chromophore at 366 nm in *n*-octane produces a 51:49 ratio of HD to BCH. Triplet-sensitized photolysis employing benzophenone in *n*-octane produces a 70:30 ratio of HD to BCH. The $^{14}N/^{15}N$ isotope effect on deazotation was measured by Anderson and Grissom[19,20] to be 1.025 for DBO and 1.004 for the more strained DBH. These data suggest that on direct photolysis cleavage of the first C−N bond in DBO occurs from the excited singlet state in a thermally activated process with a late transition state whereas C−N bond cleavage in DBH involves an early transition state.[19,20] By examining the dependence of the product distribution on the concentration of heavy-atom-containing solvents, Anderson and Grissom[19,20] found that the ratio of products can be quantitatively understood by assuming that the intersystem crossing (ISC) is rapid between the singlet and triplet states of the cyclohexane-1,4-diyl intermediate. Also, their experiments provided no evidence for ISC between the excited singlet and triplet states of DBO prior to cleavage of the first C−N bond.

Compared to the extensive experimental studies on the photolysis of DBO, related theoretical studies are still scarce. To our best knowledge, there are only two. The first one is due to Roberson and Simons,[24] who computed the potential energy surfaces (PESs) of the ground state and the lowest triplet state of DBO using Hartree−Fock and density functional methods. The reported energy of the triplet state and the activation barrier for C−N cleavage on the triplet surface were in good agreement with the corresponding experimental values. On the basis of their computed PESs, the authors of this study offered a detailed interpretation of the various experimental findings on the photolysis of DBO. However, the PESs of the singlet excited state and higher triplet states of DBO were not reported, so no attempt was made to investigate the processes of ISC or internal conversion (IC), which are crucial for understanding the photochemical behavior of DBO. The second theoretical study is from Nau et al.,[25] who used the CASPT2/CASSCF method to calculate the 0−0 singlet excitation energy (73.7 kcal/mol) and the activation barrier of the C−N cleavage (11.4 kcal/mol) on the singlet excited state. Their predictions agree well with the corresponding experimental numbers (76.4 and 8.6 kcal/mol, respectively), but again, no detailed studies of the crossing

(10) Photochemical deazotation of DBH and its derivatives: (a) Roth, W. R.; Martin, M. *Justus Liebigs Ann. Chem.* **1967**, *702*, 1. (b) Engel, P. S. *J. Am. Chem. Soc.* **1969**, *91*, 6903. (c) Bauer, S. H. *J. Am. Chem. Soc.* **1969**, *91*, 3688. (d) Buchwalter, S. L.; Closs, G. L. *J. Am. Chem. Soc.* **1975**, *97*, 3857. (e) Buchwalter, S. L.; Closs, G. L. *J. Am. Chem. Soc.* **1979**, *101*, 4688. (f) Herman, M. S.; Goodman J. L. *J. Am. Chem. Soc.* **1988**, *110*, 2681. (g) Adam, W.; Oppenlander, T.; Zang, G. *J. Org. Chem.* **1985**, *50*, 3303. (h) Simpson, C. J. S. M.; Wilson, G. J.; Adam, W. *J. Am. Chem. Soc.* **1991**, *113*, 4728. (i) Adam, W.; Nau, W. M.; Sendelbach, J.; Wirtz, J. *J. Am. Chem. Soc.* **1993**, *115*, 12571. (j) Adam, W.; Nau, W. M.; Sendelbach, J. *J. Am. Chem. Soc.* **1994**, *116*, 7049. (k) Adam, W.; Fragale, G.; Klapstein, D.; Nau, W. M.; Wirtz, J. *J. Am. Chem. Soc.* **1995**, *117*, 12578. (l) Adam, W.; Denninger, U.; Finzel, R.; Kita, F.; Platsch, H.; Walter, H.; Zang, G. *J. Am. Chem. Soc.* **1992**, *114*, 5027. (m) Adam, W.; Hossel, P.; Hummer, W.; Platsch, H.; Wilson, R. M. *J. Am. Chem. Soc.* **1987**, *109*, 7570.

(11) Engel, P. S.; Nalepa, C. J. *Pure Appl. Chem.* **1980**, *52*, 2621.

(12) Engel, P. S.; Steel, C. *Acc. Chem. Res.* **1973**, *6*, 275.

(13) Solomon, B. S.; Thomas, T. F.; Steel, C. *J. Am. Chem. Soc.* **1968**, *90*, 2249.

(14) Clark, W. D. K.; Steel, C. *J. Am. Chem. Soc.* **1971**, *93*, 6347.

(15) Engel, P. S.; Horsey, D. W.; Key, D. E.; Nalepa, C. J.; Soltero, L. R. *J. Am. Chem. Soc.* **1983**, *105*, 7108.

(16) Edmunds, A. J. F.; Samuel, C. J. *J. Chem. Soc., Perkin Trans. 2* **1989**, 1267.

(17) Mirbach, M. J.; Kou-Chang Liu; Milbach, M. F.; Cherry, W. R.; Turro, N. J.; Engel, P. S. *J. Am. Chem. Soc.* **1978**, *100*, 5122.

(18) Adam, W.; Nikolaus, A. *J. Am. Chem. Soc.* **2000**, *122*, 884.

(19) Anderson, M. A.; Grissom, C. B. *J. Am. Chem. Soc.* **1995**, *117*, 5041.

(20) Anderson, M. A.; Grissom, C. B. *J. Am. Chem. Soc.* **1996**, *118*, 9552.

(21) Caldwell, R. A.; Helms, A. M.; Engel, P. S.; Wu, A. *J. Phys. Chem.* **1996**, *100*, 17716.

(22) Engel, P. S.; Keys, D. E.; Kitamura, A. *J. Am. Chem. Soc.* **1985**, *107*, 4964.

(23) Adam, J. S.; Nau, Weisman, R. B.; Engel, P. S. *J. Am. Chem. Soc.* **1990**, *112*, 9115.

(24) Roberson, M. J.; Simons, J. *J. Phys. Chem. A* **1997**, *101*, 2379.

(25) Nau, W. M.; Greiner, G.; Wall, J.; Rau, H.; Olivucci, M.; Robb, M. A. *Angew. Chem., Int. Ed.* **1998**, *37*, 98.

(26) (a) Nau, W. M.; Zhang X. Y. *J. Am. Chem. Soc.* **1999**, *121*, 8022. (b) Uppili, S.; Marti, V.; Nikolaus, A.; Jockusch, S.; Adam, W.; Engel, P. S.; Turro, N. J.; Ramamurthy, V. *J. Am. Chem. Soc.* **2000**, *122*, 11025. (c) Zhang, X. Y.; Nau, W. M. *Angew. Chem., Int. Ed.* **2000**, *39*, 544. (d) Mayer, B.; Zhang, X. Y.; Nau, W. M.; Marconi, G. *J. Am. Chem. Soc.* **2001**, *123*, 5240. (e) Zhang, X. Y.; Gramlich, G.; Wang, X. J.; Nau, W. M. *J. Am. Chem. Soc.* **2002**, *124*, 254. (f) Marquez, C.; Hudgins, R. R.; Nau, W. M. *J. Am. Chem. Soc.* **2004**, *126*, 5806.

(27) (a) Hudgins, R. R.; Huang, F.; Gramlich, G.; Nau, W. M. *J. Am. Chem. Soc.* **2002**, *124*, 556. (b) Nau, W. M.; Wang, X. J. *J. Am. Chem. Soc.* **2004**, *126*, 808. (c) Huang, F.; Hudgins, R. R.; Nau, W. M. *J. Am. Chem. Soc.* **2004**, *126*, 16665. (d) Gramlich, G.; Zhang, J. Y.; Nau, W. M. *J. Am. Chem. Soc.* **2004**, *126*, 5482. (e) Marquez, C.; Pischel, U.; Nau, W. M. *Org. Lett.* **1999**, *5*, *3911*.

(28) (a) Nau, W. M. *J. Am. Chem. Soc.* **1998**, *120*, 12614. (b) Nau, W. M.; Pischel, U. *Angew. Chem., Int. Ed.* **1999**, *38*, 2885. (c) Pischel, U.; Zhang, X.; Hellrung, B.; Haselbach, E.; Muller, P.-A.; Nau, W. M. *J. Am. Chem. Soc.* **2000**, *122*, 2027. (d) Sinicropi, A.; Pischel, U.; Basosi, R.; Nau, W. M.; Olivucci, M. *Angew. Chem., Int. Ed.* **2000**, *39*, 4582. (e) Sinicropi, A.; Pogni, R.; Basosi, R.; Robb, M. A.; Gramlich, G.; Nau, W. M.; Olivucci, M. *Angew. Chem., Int. Ed.* **2001**, *40*, 4185. (f) Klapstein, D.; Pischel, U.; Nau, W. M. *J. Am. Chem. Soc.* **2002**, *124*, 11349.

(29) Yamamoto, N.; Olivucci, M.; Celani, P.; Bernardi, F.; Robb, M. A. *J. Am. Chem. Soc.* **1998**, *120*, 2391.

(30) Sinicropi, A.; Page, C. S.; Adam, W.; Olivucci, M. *J. Am. Chem. Soc.* **2003**, *125*, 10947.

among the low-lying excited states in the photolysis of DBO were reported.

Clearly, despite the theoretical studies described above, many important questions remain to be answered with regard to the photolysis of DBO. For example, the unusually broad emission band of DBO in the gas phase and in solution is not fully understood,[31] and it is also not clear why DBO has such an extraordinarily long-lived excited singlet state and a short-lived triplet state. In particular, the roles played by various electronic states in the photolysis of DBO are not well understood. Thus, a comprehensive theoretical study with high accuracy is required to fully understand the mechanism of the photolysis of DBO.

It is worth mentioning that the understanding of the origin of the long-lived singlet excited state of DBO is crucial for better applications of DBO and its derivatives in many fields. Due to the intense and extremely long-lived fluorescence from the lowest excited singlet state of DBO, this species was used in recent years as a novel long-lifetime fluorescent probe of high selectivity which can serve to provide structural and kinetic information on host−guest complexation in supramolecular chemistry[26,38] and the dynamics of polypeptides and nucleic acids in biochemistry and biophysics.[27] In addition, several attempts have been made to probe the quenching mechanism of the DBO singlet excited state in different solvents.[28,31,38] On the other hand, an understanding of why DBO photoeliminates nitrogen reluctantly will be necessary to design other azoalkanes, structurally analogous to DBO but with higher denitrogenation yields, which can be used to synthesize more unusual organic molecules.

In this paper we investigate the detailed potential energy surfaces of the lowest excited singlet state (S_1) and low-lying triplet states (T_1, T_2, and T_3) that are possibly involved in the photolysis of DBO by the CASPT2/CASSCF method. The energies and structures of various stationary and crossing points will provide the basis for a comprehensive picture of the photolysis mechanism of DBO. Specifically, our objectives are (a) to elucidate the origin of the extremely long-lived fluorescence from the lowest excited singlet state of DBO, and the rapid radiationless decay of the triplet state of DBO, and (b) to determine all possible reaction paths for denitrogenation on the lowest excited singlet and triplet surfaces.

2. Computational Details

The CASSCF geometry optimizations for ground-state and excited-state intermediates, transition states, singlet/singlet and triplet/triplet conical intersections, and singlet/triplet crossing points were carried out using the MCSCF program contained in the Gaussian98 package[32] with a 6-31G* basis. Conical intersections are considered as the main locus of IC, while singlet/triplet crossings are the main locus of ISC. Frequency calculations were performed for all stationary points on the potential energy surfaces to obtain zero-point energies (ZPEs) and to verify whether they are minima or transition states. Geometry optimizations of the crossing points (IC and ISC) were performed with the state-averaged CASSCF method. To include dynamic correlation energies, single-point CASPT2[33,34] calculations with the same basis set and active space were carried out at the CASSCF-optimized geometries with the MOLPRO2000 package.[35] The level shift technique was used in all CASPT2 calculations to avoid intruder state problems.[36] Spin−orbit coupling constants were calculated using the full Breit−Pauli SO operator[37] with the Molpro2000 package. In addition, for all stationary points and crossing points located, we performed single-point CASSCF and CASPT2 calculations with a larger polarized triple-ζ basis set, 6-311G*, to check the basis set dependence of the relative energies.

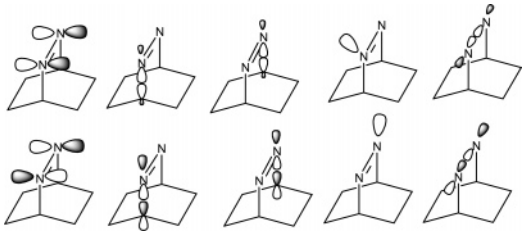

Figure 1. Active space used in our CASSCF calculations.

Figure 1 shows the active space used in all our CASSCF and CASPT2 calculations. To describe the cleavage of the two C−N bonds, one needs both pairs of C−N σ and σ^* orbitals, and six orbitals from the N_2 fragment (π, π^*, two n orbitals, σ, and σ^*). The resulting active space of 12 electrons in 10 orbitals is labeled (12,10). The σ and σ^* orbitals of N_2 are included because the N−N bond length varies significantly in the course of the deazotation. In regions of the potential energy surface near the diazenyl diradicals, the lone pair orbital of the nitrogen atom of the broken C−N bond is nearly doubly occupied in all states under study. Since the inclusion of orbitals with occupancies near 2 or 0 in the active space dramatically deteriorates the convergence of the CASSCF calculations, we deleted the N lone pair from the active space described above to form a (10,9) active space for these cases. The reduction of the active space will lead to small errors when CASSCF energies are compared for species in different regions of the PES, but after the MP2 corrections are added, the energies obtained with the two active spaces can again be compared directly.

It is important to estimate the accuracy of the method and the basis sets we use in this work. With the CASPT2/CASSCF method, the calculated singlet 0−0 energy gap of DBO is 72.3 kcal/mol at the 6-31G* level and 70.7 kcal/mol at the 6-311G* level (the ZPE corrections calculated at the CASSCF/6-31G* level are added). These values agree reasonably well with the corresponding experimental value of 76.4 kcal/mol[38] in the gas phase. Our present calculations and results from other researchers for similar systems[29,30] demonstrate that the CASPT2/CASSCF method with the 6-31G* basis set should give a reliable description of the PES of DBO and its excited states.

3. Results and Discussion

In this section, we will present the PESs of the low-lying singlet and triplet states S_0, S_1, T_1, T_2, and T_3 of DBO in four subsections. The first one includes the PESs of S_0, S_1, T_1, and T_2 near the ground-state equilibrium geometry. Then, the decay pathways from the excited singlet and triplet states are discussed. In subsections 3.2 and 3.3, we will describe the PESs of the low-lying excited states in the region where the first C−N bond is broken, and in the vicinity of the resulting diazenyl diradicals. Finally, a comparison of our theoretical results with the available experimental results will be made in subsection 3.4. The optimized geometries of all stationary points and crossing points (ISC or IC) are shown in Figure 2, and their relative energies are collected in Table 1. As seen from Table 1, the relative energies obtained from single-point CASPT2 calculations at the

(31) Nau, W. M.; Greiner, G.; Wall, J.; Rau, H.; Wall, J.; Olivucci, M.; Scaiano, J. C. *J. Phys. Chem. A* **1999**, *103*, 1579.
(32) Frisch, M. J.; et al. *Gaussian98*, revision A.9; Gaussian, Inc.: Pittsburgh, PA, 1998.
(33) Werner, H. J. *Mol. Phys.* **1996**, *89*, 645.
(34) Celani, P.; Werner, H. J. *J. Chem. Phys.* **2000**, *112*, 5546.
(35) Werner, H. J.; Knowles, P. J. *MOLPRO* (a package of ab initio programs), version 2000.1; University of Birmingham: Birmingham, U.K., 1999.
(36) Roos, B. O.; Andersson, K. *Chem. Phys. Lett.* **1995**, *245*, 215.
(37) Berning, A.; Schweizer, M.; Werner, H. J.; Knowles, P. J.; Palmieri, P. *Mol. Phys.* **2000**, *98*, 1823.
(38) Marquez, C.; Nau, W. M. *Angew. Chem., Int. Ed.* **2001**, *40*, 4387.

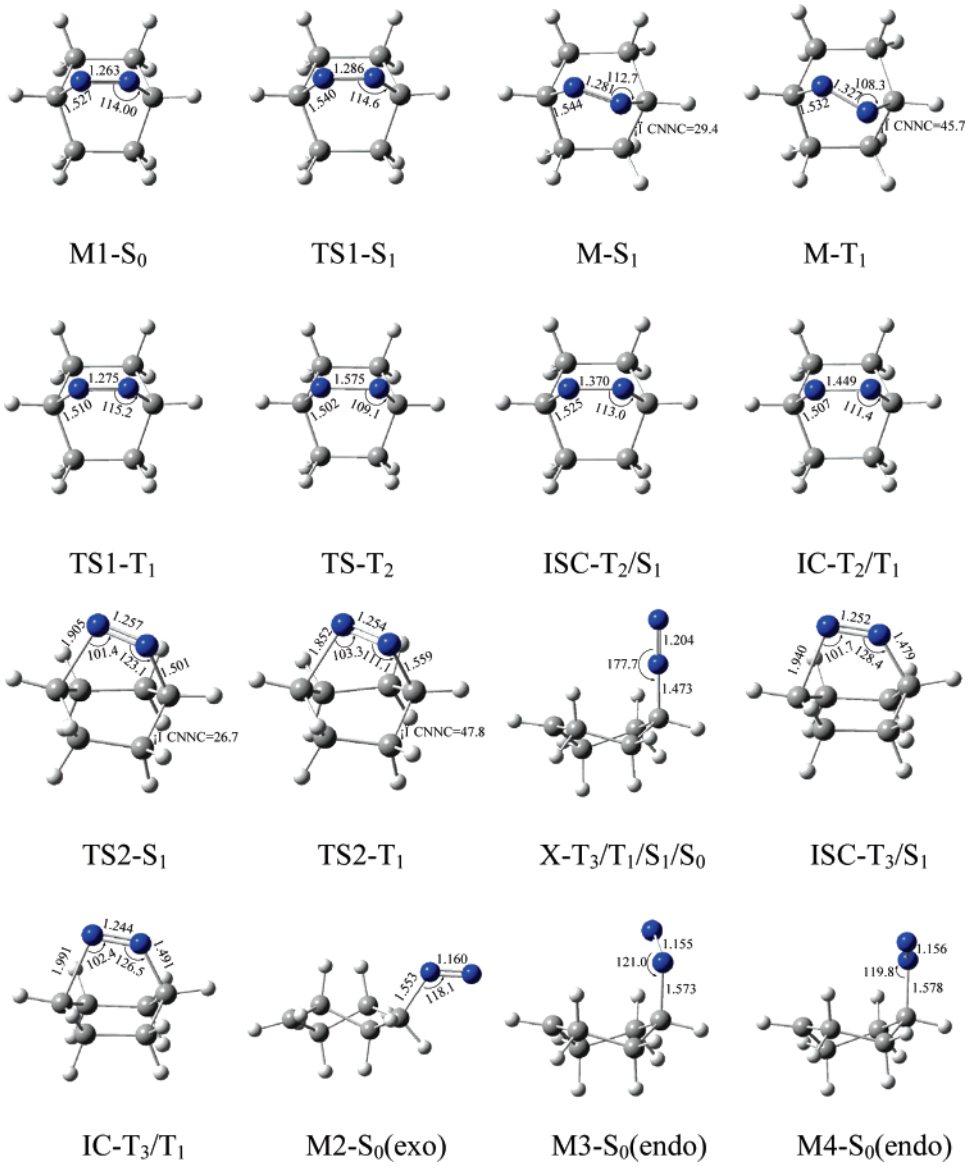

Figure 2. CASSCF-optimized geometries of the minima, transition states, and crossing points for intersystem crossing (ISC) and internal conversion (IC).

6-31G* level are very close to those at the 6-311G* level, with the largest deviation being less than 3.0 kcal/mol. Thus, the calculated relative energies exhibit only a small basis set dependence. Unless stated otherwise, the relative energies from CASPT2/6-31G* calculations will be used in subsequent discussions. Some calculated results that can be directly compared with experimental values are listed in Table 2.

3.1. Excited-State PESs near the Ground-State Equilibrium Geometry. 3.1.1. Stationary Points. As shown in Figure 2, the ground-state minimum, M1-S_0, of DBO is of C_{2v} symmetry, with the N−N bond and C−N bond lengths being 1.263 and 1.527 Å, respectively. After including dynamic correlation by single-point CASPT2 calculations, the vertical excitation energies for S_0-T_1, S_0-S_1, and S_0-T_2 are calculated to be 59.0, 76.7, and 114.6 kcal/mol, respectively, as shown in Table 1. Thus, on direct photolysis at 366 nm (78.1 kcal/mol) and triplet-sensitized photolysis at 313 nm (91.3 kcal/mol), only the T_1 and S_1 states are accessible. In the Franck−Condon region of the S_1 (n−π*) surface, we located a stationary point of C_{2v} symmetry with r(N−N)= 1.286 Å. Our vibrational analysis indicated that this point is a transition state (TS1-S_1), in which the imaginary vibrational mode corresponds to the twisting of the C−N═N−C bridge. By following the transition vector of TS1-S_1, we found a minimum (M-S_1) of C_2 symmetry, about 2.3 kcal/mol below TS1-S_1, with a C−N═N−C dihedral angle of 29.4°. So the C_{2v} symmetrical transition state TS1-S_1 links the minimum M-S_1 and its enantiomer, as shown in Scheme 2. On twisting the C−N═N−C bridge, the n and π orbitals of the N−N moiety slightly mix in the S_1 state. Interestingly, for DBH, which is slightly more rigid than DBO, a C−N═N−C twisted minimum was found to exist only on the T_1 state but not on the S_1 state.[29]

The twisting distortion of the S_1 (n−π*) state from its "native" C_{2v} symmetry, where it is a $^1B_1$ state, occurs along a coordinate of a_2 symmetry. According to the rules that govern vibronic interactions,[39,40] this twisting may be induced by

(39) Bersuker, I. B. *The Jahn-Teller Effect and Vibronic Interactions in Modern Chemistry*; Plenum Press: New York, 1984; p 61.
(40) (a) Köppel, H.; Domcke, W.; Cederbaum, L. S.; Shaik, S. S. *Angew. Chem., Int. Ed. Engl.* **1983**, *22*, 210. (b) Köppel, H.; Domcke, W.; Cederbaum, L. S. *Adv. Chem. Phys.* **1984**, *57*, 59.

Table 1. Calculated CASSCF and CASPT2 Energies of Stationary Points and Crossing Points on the Low-Lying Surfaces of DBO

		relative energy[b] (kcal/mol)		
geometry	state	CASSCF (6-31G*)	CASPT2 (6-31G*)	CASPT2[c] (6-311G*)
M1-S_0	S_0	0.0	0.0	0.0
	T_1 (n−π*)	78.5	59.0	57.9
	T_2 (π−π*)	124.5	114.6	113.7
	S_1 (n−π*)	96.1	76.7	75.2
TS1-S_1	S_1 (n−π*)	94.9	76.1 (74.0)	74.8 (72.7)
M-S_1	S_1 (n−π*)	93.9	73.8 (72.3)	72.2 (70.7)
M-T_1	T_1 (n−π*−π−π*)	66.2	51.3 (50.0)	50.5 (49.2)
TS1-T_1	T_1 (n−π*)	75.5	56.2 (54.7)	55.2 (53.7)
TS-T_2	T_1 (π−π*)	86.5	80.3 (78.0)	80.8 (78.5)
ISC-T_2/S_1	T_2 (π−π*)	100.7	91.7	91.4
	S_1 (n−π*)	100.7	81.1	80.2
IC-T_2/T_1	T_2 (π−π*)	92.2	83.0	83.2
	T_1 (n−π*)	92.2	72.5	72.0
TS2-S_1	S_1 (n−π*)	99.0	86.0 (83.2)	84.6 (81.8)
TS2-T_1	T_1 (n−π*−π−π*)	72.7	62.2 (59.0)	60.8 (57.6)
X-T_3/T_1/S_1/S_0	S_0	76.6	76.6	75.1
	S_1 (n−π*)	77.2	77.4	76.1
	T_1 (n−π*)	77.1	77.6	76.1
	T_2 (n−σ*)	77.2	77.6	76.1
IC-T_3/T_1	T_1 (n−π*)	96.9	81.5	79.9
	T_2 (n−σ*)	96.9	90.7	88.9
ISC-T_3/S_1	S_1 (n−π*)	107.7	91.5	89.7
	T_2 (n−σ*)	107.7	99.6	97.5
M2-S_0(exo)[a]	S_0	41.0	49.1	46.4
M3-S_0(endo)[a]	S_0	40.0	48.4	45.6
M4-S_0(endo)[a]	S_0	41.1	49.2	46.4

[a] The structures are optimized at the CASSCF(4,4) level. [b] The ZPE-corrected energies are included in parentheses. [c] The ZPE corrections calculated at the CASSCF/6-31G* level are added.

Table 2. A Comparison of Calculated and Experimental Excitation Energies and Activation Energies of DBO

param[a]	present study[b]	expl	other theoretical values
E_S	73.8 (72.3)	76.4[c]	73.7[f]
E_T	51.3 (50.0)	51.9 ± 0.6[d]	53[g]
E_a^D	12.2 (10.9)	8.6[e]	11.4[f]
E_a^S	10.9 (9.0)	9.0[e]	

[a] E_S and E_T stand for the energies of the S_1 and T_1 states, respectively; E_a^D and E_a^S are the activation energies on the S_1 and T_1 states, respectively. [b] ZPE-corrected energies at the 6-31G* level are included in parentheses. [c] Reference 38. [d] Reference 21. [e] Reference 15. [f] Reference 25. [g] Reference 24.

vibronic coupling to a state of B_2 symmetry, in close analogy to the recently described case of the bicyclo[2.2.2]oct-2-ene radical cation.[41] This twisting appears to be an inherent property of the n−π* excited azo chromophore, as it has been shown to occur also in *cis*-diimide (H−H═N−H) and *cis*-azomethane (Me−N═N−Me).[42] The π−π* excited states of *cis*-azo moieties have the proper symmetry ($^1B_2$) to induce an a_2 distortion of their $^1B_1$ n−π* excited states, and the observed slight mixing of the n and π MOs at the twisted minimum structure M-S_1 of DBO indicates that the π−π* excited state may indeed be responsible for the twisting of DBO in its S_1 n−π* state. Our calculations show that the π−π* state lies quite high in energy and is not even the lowest one of its symmetry. However, if the integral that describes the coupling between the n−π* and π−π* excited states (the so-called derivative coupling integral) is large, then it may outweigh a large ΔE denominator in the expression describing the extent of vibronic interaction.[39,40]

Scheme 2

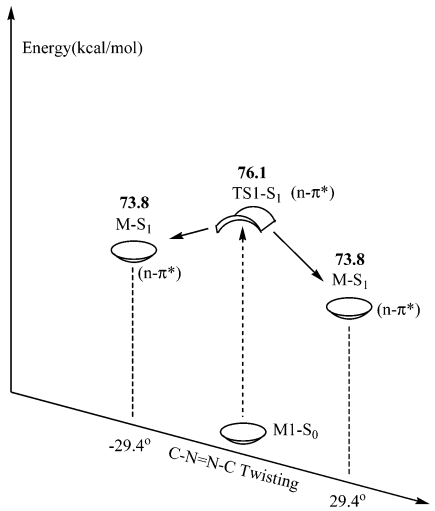

If the azo group forms part of a bicyclic framework, as in DBO and DBH, that part of the molecule may undergo an increase in strain that opposes the twisting. Obviously this increase in strain is not large enough to prevent the twisting in the n−π* excited DBO, but the more rigid DBH frame is apparently capable of achieving this effect.

The twisting of the C−N═N−C bridge can explain well the broad envelope of the DBO emission band. The vertical emission energy from M-S_1 to the ground state S_0 is 62.7 kcal/mol at the CASPT2/6-31G* level. This value agrees very well with the 444 nm (64.4 kcal/mol)[38] maximum in the gas-phase DBO emission spectrum. The absence of vibrational structure in this band can be explained by the higher density of the vibrational level in the region of the twisted C−N═N−C bridge on the S_0 surface. The energy difference between the ground state at its equilibrium geometry and that at the geometry of M-S_1 was calculated to be 11.1 kcal/mol, which accounts quite well for the half-width (about 10 kcal/mol) of the emission band.

Now let us turn to the triplet states, where already the second excited state, T_2, is of π−π* nature. We located two stationary points of C_{2v} symmetry, TS1-T_1 and TS-T_2. The main difference between these two geometries is that the N−N bond length is much longer in TS-T_2 (1.575 Å) than in TS1-T_1 (1.275 Å). The imaginary vibrational modes at both saddle points correspond again to a twisting of the C−N═N−C bridge which is, however, much more pronounced than that in the S_1 state in that the dihedral angle at the resulting minimum M-T_1 is 45.7° and the stabilization amounts to 4.9 kcal/mol, relative to TS1-T_1.[43] It should be pointed out that the energy ordering of these two triplet states is reversed when the geometry of the molecule changes from TS1-T_1 to TS-T_2; i.e., the T_2 (π−π*) state lies 55.1 kcal/mol above the n−π* state TS1-T_1, whereas it lies 12.9 kcal/mol below the n−π* state at TS-T_2, all at the CASPT2 level.

The mixing between n and π MOs is much more pronounced in M-T_1 than in M-S_1; i.e., the resulting state cannot be classified as n−π* or π−π*.[43] This, and the much larger distortion in T_1

(41) Nelsen, S. F.; Reinhardt, L. A.; Tran, H. Q.; Clark, T.; Chen, G. F.; Pappas, R. S.; Williams, F. *Chem.—Eur. J.* **2002**, *8*, 1074.
(42) (a) Kim, K.; Shavitt, I.; Del Bene, J. E. *J. Chem. Phys.* **1992**, *96*, 7573. (b) Hu, C.-H.; Schaefer, H. F., III *J. Phys. Chem.* **1995**, *99*, 7507. (c) Liu, R.-F.; Cui, Q.; Dunn, K. M.; Morokuma, K. *J. Chem. Phys.* **1996**, 105, 2333.

(43) The same minimum, M-T_1, is attained from TS1-T_1 and from TS-T_2.

Scheme 3

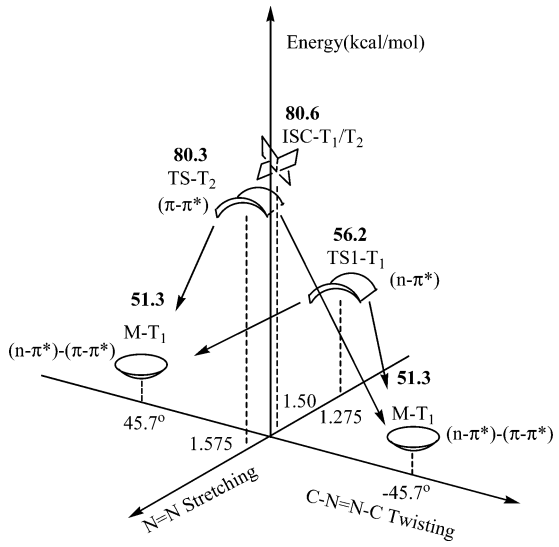

compared to S_1, supports the hypothesis that it is indeed the coupling of n$-\pi^*$ with the $\pi-\pi^*$ excited state that induces the twisting of the C—N═N—C bridge. If we assume that the derivative coupling integral is the same in both spin states, then the extent of vibronic mixing is inversely proportional to the n$-\pi^*/\pi-\pi^*$ energy difference, which is obviously much smaller in the triplet than in the singlet manifold, because the singlet−triplet splitting is much larger in $\pi-\pi^*$ than in n$-\pi^*$ states.Given the energies of M-S_1 and M-T_1, one can conclude that the calculated 0−0 energies for the S_0-S_1 and the S_0-T_1 transitions are 73.8 and 51.3 kcal/mol, respectively, at the CASPT2 level. These values are in excellent agreement with the experimental 0−0 transition energies of 76.4 kcal/mol[38] and 51.9 ± 0.6 kcal/mol,[21] respectively. The highly twisted triplet minimum, M-T_1, is predicted to lie only 22.7 kcal/mol above S_0. Caldwell et al.[21] have suggested that the closeness of the S_0 and T_1 states induced by twisting the C—N═N—C bridge in DBO may be responsible for the fast radiationless $T_1 \rightarrow S_0$ decay in DBO. Clearly, this argument finds support from the present results.

From the above results, one can see that, due to vibronic coupling with the $\pi-\pi^*$ states, the n$-\pi^*$ excited-state surfaces S_1 and T_1 exhibit the characteristics of transition states in the Franck−Condon region. After vertical excitation to S_1 DBO will relax to the twisted minimum M-S_1, while on triplet-sensitized excitation to T_1 DBO will relax to the even more twisted minimum M-T_1.

3.1.2. Crossing Points. Now we will explore the IC and ISC processes near the S_0 equilibrium geometry as possible decay mechanisms for the low-lying excited states.

First, our state-averaged CASSCF(12,10) optimization resulted in a T_2 ($\pi-\pi^*$)/S_1 (n$-\pi^*$) crossing point, ISC-T_2/S_1, 6.8 kcal/mol above the S_1 minimum, M-S_1. The geometry of ISC-T_2/S_1 is of C_{2v} symmetry with an N−N distance of 1.370 Å, slightly longer than that of M-S_1 (1.281 Å). Thus, by stretching the N−N bond, and by straightening the C—N═N—C bridge, the molecule can reach this crossing point from M-S_1. However, the spin−orbit coupling (SOC) value at ISC-T_2/S_1 is calculated to be only 6.4 cm^{-1}, so spin flip between the S_1 (n$-\pi^*$) and T_2 ($\pi-\pi^*$) states may be possible but is not expected to be very efficient. After direct irradiation in the gas phase, especially at low pressure where excessive vibrational energy cannot be readily dissipated, DBO may actually access the ISC-T_2/S_1 structure and undergo intersystem crossing, in contrast to that in solution, where the excess energy is not available long enough to sustain that process. This may explain the observed high quantum yield for deazotation via the triplet state in the gas phase,[14] whereas DBO is a very "reluctant" source of N_2 in solution.[15]

On the other hand, intersystem crossing between the S_1 (n$-\pi^*$) and T_1 (n$-\pi^*$) states, which are separated by at least 16 kcal/mol at all geometries that we examined (cf. Figure 3), is forbidden by El-Sayed's rules;[44] hence, direct ISC between these two states should be very inefficient, if not impossible, in DBO. Thus, S_1/T_2 ISC, followed by rapid T_2/T_1 internal conversion, appears to be the only viable mechanism for formation of triplet DBO after S_0-S_1 excitation.

Second, we found a conical intersection between the T_2 ($\pi-\pi^*$) and T_1 (n$-\pi^*$) states, labeled IC-T_2/T_1, 5.7 kcal/mol above TS-T_2. This point is also of C_{2v} symmetry, but the N−N bond length is 1.449 Å, compared to 1.370 Å in ISC-T_2/S_1.

It should be noticed that the degeneracy of the T_2 and S_1 states at ISC-T_2/S_1 (and that of the T_2 and T_1 states at IC-T_2/T_1) obtained at the CASSCF level is lifted after the MP2 corrections are added to the CASSCF energies of two crossing states. Thus, it is to be expected that dynamic correlation has a strong effect on the geometries of these two crossing points. In principle, one should optimize the structures of these two crossing points by the CASPT2 method, but unfortunately this kind of optimization is not feasible yet for systems as large as DBO. Instead, we employed an approximate approach. We noticed that the relative energies of the T_1 (n$-\pi^*$), T_2 ($\pi-\pi^*$), and S_1 (n$-\pi^*$) states are mainly affected by the N−N bond length, as shown by the CASSCF-optimized geometries of these species. Thus, we carried out a series of constrained CASSCF optimizations by fixing the N−N bond length at different values, and performed single-point CASPT2 calculations at the resulting geometries to correct the energetics. The results are shown in Figure 3. The structures of ISC-T_2/S_1 and IC-T_2/T_1 obtained from full CASSCF optimizations are well reproduced by the constrained optimizations, which confirm that the N−N bond distance is a good indicator of the relative energies of these excited states in this crossing region. After the MP2 correlation energies are added, the T_2/S_1 intersystem crossing is predicted to occur at r(N−N) = 1.42 Å and the conical intersection (T_2/T_1) is predicted to be located at r(N−N) = 1.50 Å. Correspondingly, the energies of ISC-T_2/S_1 and IC-T_2/T_1 at the CASPT2 level are about 86 and 80 kcal/mol, respectively, above the ground-state minimum. So at the CASPT2 level the energy required to climb from the S_1 minimum, M-S_1, to the S_1/T_2 crossing point, ISC-T_2/S_1, is about 12.2 kcal/mol.

It should be pointed out that two vibrational modes are important in the excited-state evolution of DBO. These two modes are the N═N stretching and the C—N═N—C twisting. The former leads to the crossing between the pure n$-\pi^*$ and $\pi-\pi^*$ states, and the latter causes these two states to mix. In contrast, in DBH the N═N—C antisymmetric bending (instead of the N−N stretching in DBO) was found to be responsible for the crossing between the n$-\pi^*$ and $\pi-\pi^*$ states, while the

(44) See, e.g.: Turro, N. J. *Modern Molecular Photochemistry*; Benjamin Cummings: Menlo Park, CA, 1978; pp 165−169.

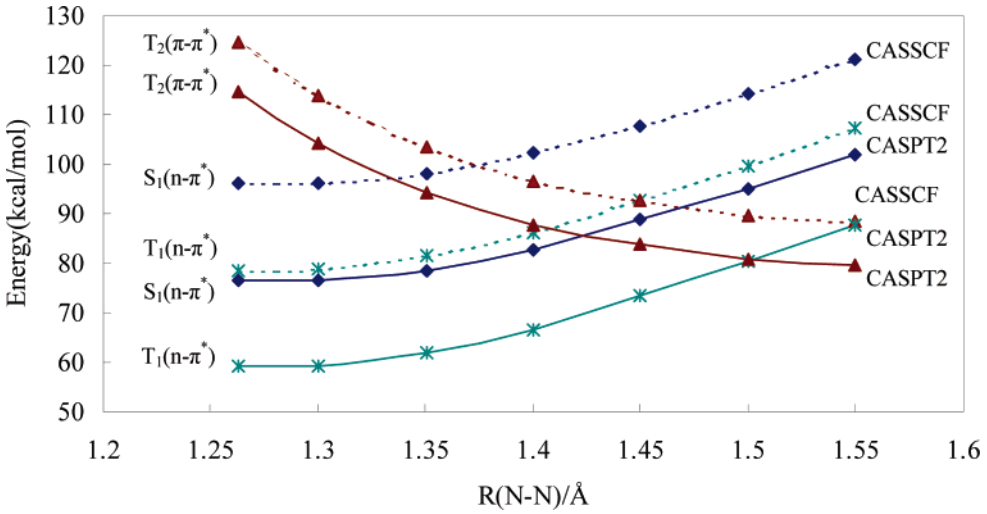

Figure 3. CASSCF and CASPT2 energies of the T_1 (n−π*), T_2 (π−π*), and S_1 (n−π*) states as a function of the N−N bond distance.

Scheme 4

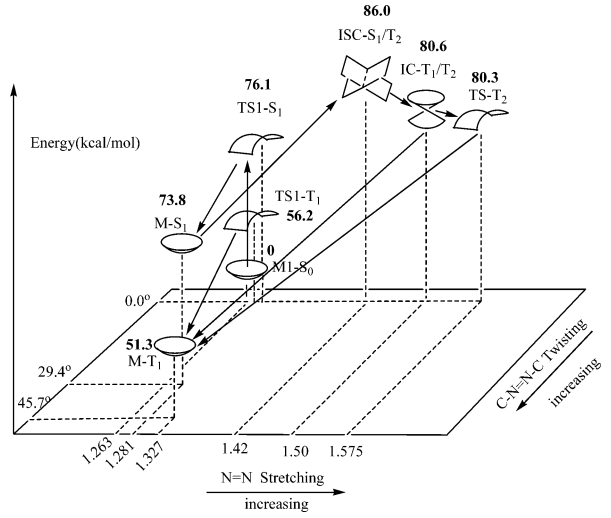

C−N═N−C distortion has a similar effect.[29] In summary, our results on the excited-state PESs near the ground-state equilibrium geometry are presented schematically in Scheme 4.

3.2. Excited-State PESs in the C−N Breaking Region. 3.2.1. Stationary Points. On the S_1 surface, we have located a transition state, labeled TS2-S_1, which corresponds to an asynchronous C−N ring-opening process. It links M-S_1 on one side to a 4-fold crossing point (see the discussion below) on the other side. In TS2-S_1, the C−N bond distance is 1.905 Å, indicating that this bond is being broken. At the CASPT2 level, the calculated activation energy for the C−N cleavage is 10.9 kcal/mol, including ZPE corrections. This result agrees well with the experimental value of 8.6 kcal/mol[15] in benzene and with the previous theoretical value of 11.2 kcal/mol.[25] The ^{15}N kinetic isotope effect showed that the C−N cleavage transition state on the S_1 surface is later in DBO than in DBH.[19] This is in accord with the calculated C−N bond lengths, 1.905 Å in TS2-S_1 and 1.79 Å in the corresponding transition state of DBH.[29]

We also found a corresponding C−N ring-opening transition state, TS2-T_1, on the T_1 surface, with a C−N bond distance (1.852 Å) that is slightly shorter than that in TS2-S_1, but close to that in the T_1 C−N ring-opening transition state of DBH (1.85 Å).[29] At the CASPT2 level, the activation energy for C−N cleavage from the twisted triplet minimum, M-T_1, is predicted to be 9.0 kcal/mol, including ZPE corrections. This result is in excellent agreement with the experimental value of 9.0 kcal/mol.[15]

3.2.2. Two-Fold Crossing Points. Near the transition state for C−N ring-opening, we also found a crossing point, ISC-T_3/S_1, between the T_3 (n−σ*) and the S_1 (n−π*) states, and a conical intersection, IC-T_3/T_1, between T_3 (n−σ*) and T_1 (n−π*). Both points are of C_s symmetry (the C−N═N−C bridge is not twisted) and have long C−N bond lengths, 1.940, and 1.991 Å, respectively. T_3 has n−σ* character because an electron in the N lone pair orbital must be promoted to the C−N antibonding orbital to break the C−N bond. Due to the high energy of the C−N σ* orbital, near the ground-state minimum of DBO the ^{3}(n−σ*) state lies much higher in energy than the ^{3}(π−π*) state, but when the C−N bond is elongated, it eventually falls below the ^{3}(π−π*) state. Thus, it is the T_3 (n−σ*) state rather than the T_2 (π−π*) state that is involved in the C−N cleavage process and becomes one of the four states at the 4-fold crossing point, as discussed below.

3.2.3. Four-Fold Crossing Point. On further stretching of the C−N bond, we found an approximate 4-fold crossing point of T_1, T_3, S_0, and S_1, denoted as X-$T_3/T_1/S_1/S_0$. At first, we located two conical intersections (T_3/T_1 and S_1/S_0, respectively) at the CASSCF(10,9) level,[45] and then we found that these two points are nearly degenerate and correspond to almost the same geometry, thus indicating the existence of a 4-fold crossing point. As shown in Figure 2, the structure of X-$T_3/T_1/S_1/S_0$ is characterized by a nearly linear N−N−C moiety and a twisted boat conformation of the six-membered ring. We notice that this structure is very similar to the structure of the 4-fold crossing point that was obtained previously for DBH (except that there the six-membered ring is replaced by a five-membered ring). The electron configurations of the four states that are degenerate at the 4-fold crossing point are shown schematically in Figure 4.

A common feature of these four states is that an unpaired electron from the C−N homolytic cleavage occupies an sp hybrid orbital located on a carbon atom while the other unpaired

(45) The (10,9) active space is obtained from the (12,10) active space described in the text by removing the doubly occupied lone pair orbital of the N atom of the broken C−N bond.

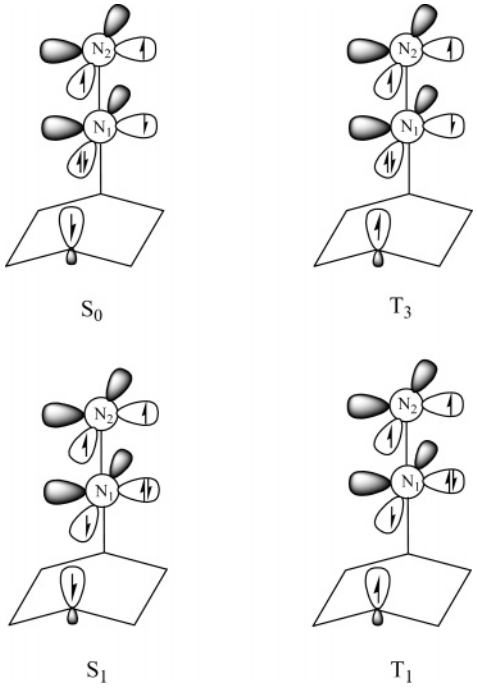

Figure 4. A schematic picture of the four states' electron configurations at the 4-fold crossing point.

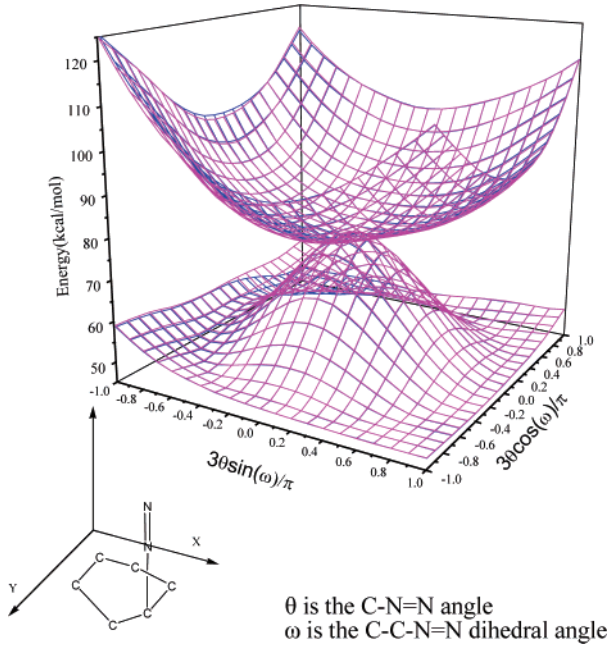

Figure 5. Potential energy surfaces of the four states near the 4-fold crossing point calculated by the CASSCF(10,9) method.

Scheme 5

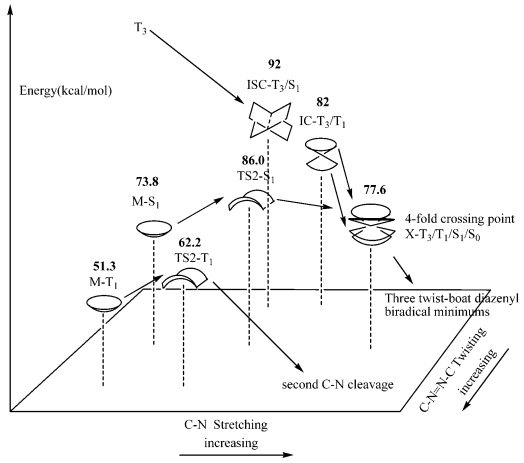

electron enters one of the two π^* orbitals of the N−N fragment. The difference between S_0 and S_1 is that in S_0 this singly occupied N−N π^* orbital is coplanar with the carbon radical orbital whereas it is perpendicular in S_1. The two unpaired electrons are antiferromagnetically coupled in S_0 and S_1, but ferromagnetically coupled in the T_1 and T_3 states. Since the two radical centers are well separated and the two π^* orbitals of the N−N moiety are nearly degenerate, the four states S_0, S_1, T_1, and T_3 have nearly identical energies at the 4-fold crossing point.

In Figure 5, we show the potential energy surfaces in two-dimensional space (one is the CNN bending; another is the CC−NN torsion) around the 4-fold crossing point. The T_1 and S_1 states on the upper sheet, as well as the T_3 and S_0 states on the lower sheet, are nearly degenerate in the vicinity of the 4-fold crossing point. The SOC value between singlet and triplet surfaces with different electronic configurations is calculated to be 20.5 cm^{-1} for S_0 and T_1 and 23.5 cm^{-1} for S_1 and T_3, but the SOC values between surfaces of the same electronic configurations are found to be much smaller (4.2 cm^{-1} for S_0 and T_3 and 11.8 cm^{-1} for S_1 and T_1). Thus, the results obtained here for DBO are analogous to the situation in DBH. The calculated SOC values imply that ISC conversion between singlet and triplet surfaces with different electronic configurations is likely to occur. On the other hand, since IC via the conical intersections is efficient, the molecule can also decay to the S_0 surface along the S_1 reaction coordinate, leading to S_0 diazenyl biradicals. To conclude, the excited-state PESs in the C−N bond breaking region are presented in Scheme 5.

3.3. Excited-State PESs in the Diazenyl Biradical Region. As discussed above, after the 4-fold crossing point the S_1 state will relax to the S_0 surface or the T_1 surface to form singlet or triplet diazenyl biradicals. On the S_0 surface, we have located three conformational minima for the diazenyl biradical (M2-S_0, M3-S_0, M4-S_0) by CASSCF calculations in a reduced active space (4,4).[46] At the CASPT2 level, the energies of these three species are all about 49 kcal/mol above the ground-state minimum, M1-S_0.

These three species can be interconverted by rotating the N−N moiety around the C−N bond. As pointed out for structurally similar diazenyl biradicals in DBH, the S_0 PES in the diazenyl biradical region is very flat; i.e., the above rotation is almost unhindered. The same should apply also for DBO. Our calculations also showed that the barriers for nitrogen extrusion from these S_0 diazenyl biradicals are all less than 3 kcal/mol at the CASPT2 level. These results are consistent with the previous theoretical results on thermal deazotation of DBO.[47] Thus, once the molecule enters the diazenyl biradical region on the S_0 surface, the nitrogen extrusion should follow readily.As discussed previously for DBH, the corresponding T_1 PES in the diazenyl biradical region for DBO is also found to be

(46) The (4,4) active space consists of two radical orbitals (centered at the C and N atoms of the broken C−N bond) and σ and σ^* orbitals of the intact C−N bond.
(47) Khong, K. S.; Houk, K. N. *J. Am. Chem. Soc.* **2003**, *125*, 14867.

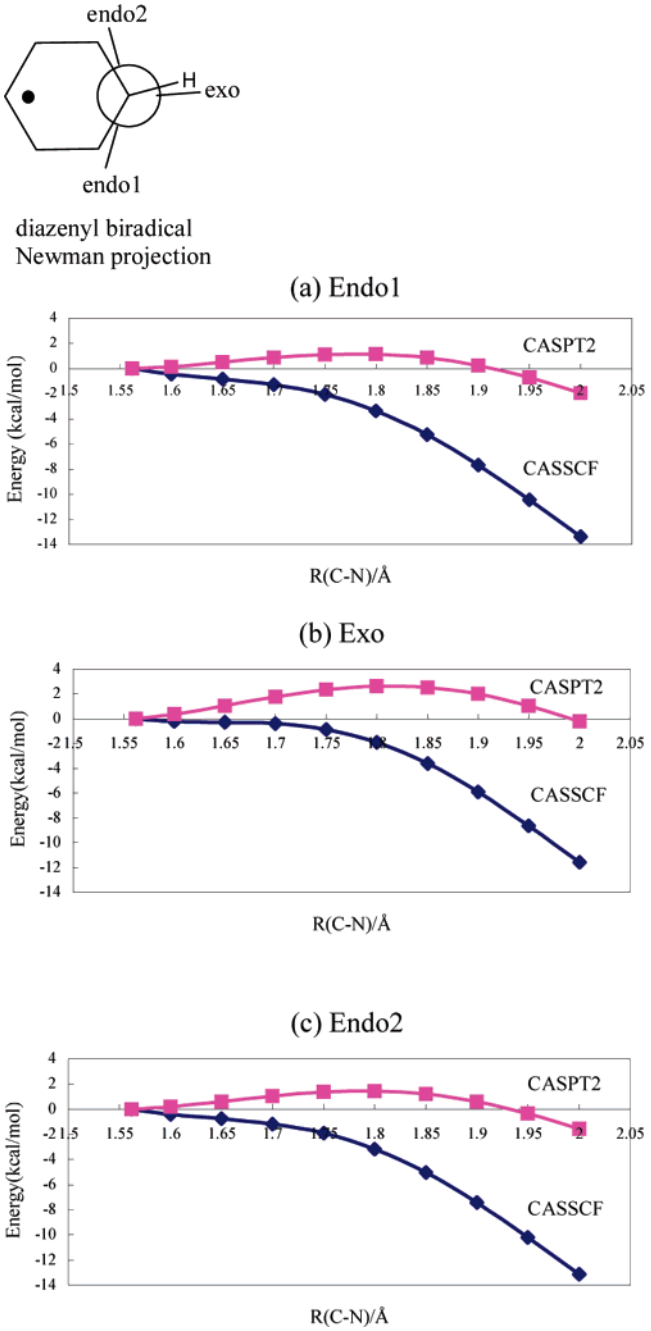

Figure 6. CASSCF and CASPT2 energy profiles of three singlet diazenyl biradicals along the reaction coordinate of denitrogenation.

extremely flat; thus, it will be omitted here. Similarly, the loss of N_2 from the T_1 diazenyl biradicals is expected to occur in a nearly barrierless fashion for DBO. On the other hand, it should be noted that the S_0 and T_1 surfaces are nearly degenerate along the reaction coordinate linking the 4-fold crossing point to the diazenyl biradical minima. Since ISC between the S_0 and T_1 diazenyl biradicals (say M2-S_0 and its T_1 state) is predicted to be relatively efficient, both singlet and triplet 1,4-cyclohexadiyl diradicals can be produced by direct photolysis.

As described above, on the T_1 surface DBO may also go via TS2-T_1 to enter the diazenyl biradical region directly, i.e., without passing through the 4-fold crossing point. In this case, our CASSCF calculations along the transition vector (the C−N stretching) showed that after the cleavage of the first C−N bond the second C−N bond is spontaneously broken, producing N_2 and a triplet 1,4-cyclohexadiyl diradical of twisted boat conformation directly. In summary, one can see that the cleavage of the first C−N bond is the rate-limiting step in the photolysis of DBO, which agrees with the previous experimental results.[19]

Once the singlet and triplet 1,4-cyclohexadiyl diradicals are formed, they will generate final products HD and BCH. The mechanisms of these transformations have been discussed in detail by Roberson and Simons,[24] and thus will be omitted here.

3.4. Comparison of Calculated Results with Experimental Data. Now we will try to elucidate the nature of the metastable excited-state species detected during direct irradiation and triplet-sensitized irradiation of DBO in the gas phase. Clearly, the excited singlet species with a lifetime of 434 ns should be assigned to the twisted singlet minimum, M-S_1. From this minimum, the DBO molecule may evolve along three different pathways. The first way is to cross to the T_2 surface via the ISC-T_2/S_1 point and subsequently decay to the T_1 surface via IC-T_2/T_1 by expanding the N−N bond length. In this step the system is required to surmount a barrier of 12.2 kcal/mol. The second way is to pass over the C−N ring-opening transition state TS2-S_1 to arrive at the 4-fold crossing point. The calculated ZPE-corrected barrier for this C−N cleavage is 10.9 kcal/mol, in good agreement with the experimental value of 8.6 kcal/mol.[15] The third way is radiative deactivation. Since both chemical deactivation pathways have relatively high barriers, the observed high quantum yield for fluorescence (0.56 ± 0.10 in the gas phase) and the very long lifetime of the DBO singlet state can be satisfactorily explained.

The calculated S_0−S_1 0−0 transition energy is 73.8 kal/mol, which is very close to the experimental value of 76.4 kcal/mol.[38] The calculated vertical S_1−S_0 emission energy is 62.7 kcal/mol, in excellent accord with the experimental 444 nm (64.4 kcal/mol)[38] maximum in the DBO emission spectrum. The broad envelope of the DBO emission band can be ascribed to the twisted structure of M-S_1 because at this geometry the S_0 surface is characterized by high vibrational levels with small energy intervals.

On the basis of our calculations and experimental results, the metastable triplet species produced by triplet sensitization can be assigned to the highly twisted minimum M-T_1. There are several pieces of evidence to support this assignment. After ZPE correction, the T_1 state lies 50.0 kcal/mol above the ground-state minimum, which compares well with the experimental value of 51.9 ± 0.6 kcal/mol.[21] Experimentally, triplet DBO decays to S_0 or undergoes deazotation, but it does not phosphoresce. According to our calculations, the minimum M-T_1 may (1) cross the IC-T_2/T_1 and subsequently the ISC-T_2/S_1 point to the S_1 surface, (2) proceed through the ring-opening transition state TS2-T_1 to directly lose nitrogen, and (3) undergo radiationless decay to return to the ground state. Our calculations tell us that the energy required to reach the conical intersection IC-T_2/T_1 is prohibitive (28.7 kcal/mol) whereas the ZPE-corrected activation barrier for breaking the C−N bond is 9.0 kcal/mol, which is identical to the experimental value measured in benzene.[15] As the energy required for the IC and subsequent ISC is much higher than the barrier for nitrogen loss, the observation that the yield of deazotation products increases significantly when one uses higher energy sensitizers in the gas phase[14] can be easily understood. On the other hand, since the

vertical emission energy from the twisted minimum M-T_1 to the ground state is calculated to be only 22.7 kcal/mol, and the rate for ISC is expected to increase with the square of this energy gap,[48] radiationless decay back to the ground state is highly probable.

Clearly, the narrowing of the S_0/T_1 gap in DBO is caused mainly by the high twisting of the C−N═N−C bridge in M-T_1. Thus, fast radiationless decay may be responsible for the very short lifetime of the triplet DBO (25 ns).[21] In addition, the lack of phosphorescence in the triplet DBO may be due to the large structural difference between M-T_1 and the ground-state minimum, which may lead to very small Franck−Condon factors.

Regarding the possibility of intersystem crossing between different electronic excited states in DBO, the long fluorescence lifetime of DBO[19,20] indicates that ISC from the S_1 state is insignificant, whereas it may be quite efficient once the molecule enters the diazenyl biradical region. These observations can also be accounted for by the present calculations. As described above, DBO S_1 can reach the triplet-state surface via two different pathways. The first one leads through the 4-fold crossing point X-$T_3/T_1/S_1/S_0$ to decay to T_1. However, to reach the 4-fold crossing point, DBO S_1 must transcend TS2-S_1, which involves a barrier of 10.9 kcal/mol. The second pathway is to undergo ISC via ISC-T_2/S_1 and IC via IC-T_2/T_1 to generate the twisted minimum M-T_1, which requires 12.2 kcal/mol of activation energy. In addition, since the calculated SOC value is only 6.4 cm^{-1} at ISC-T_2/S_1, ISC from the S_1 ($n-\pi^*$) state to the T_2 ($\pi-\pi^*$) state through the second pathway is predicted to be inefficient. In contrast, our results predict efficient ISC via the 4-fold crossing point. Thus, under direct irradiation both singlet and triplet 1,4-cyclohexadiyl diradicals can be produced.

4. Conclusions

In this paper we have used the CASPT2/CASSCF method to study the mechanism of the photolysis of DBO. By exploring the S_1, T_1, T, and T_3 potential energy surfaces near the S_0 equilibrium structure and in the region for C−N cleavage, we are able to present a comprehensive picture of the photophysical and photochemical processes of DBO under direct and triplet-sensitized irradiation. On the basis of the energies and structures of the minima, transition states, and crossing points, we can draw the following conclusions: (1) The broad envelope of the DBO emission spectrum observed experimentally is caused by relaxation along the C−N═N−C twisting mode on the S_1 excited-state surface. (2) The fast radiationless decay of triplet DBO to the ground state originates from a narrowing of the S_0/T_1 gap, which results from the relaxation of the T_1 state to a highly twisted structure. (3) From the S_1 state, ISC to the T_1 state is inefficient due to the presence of a barrier of about 12 kcal/mol and a small spin−orbit coupling constant. This fact, along with a relatively large activation barrier for C−N cleavage on the S_1 surface, may account for the very long lifetime of the first singlet excited state and its high fluorescence quantum yield. (4) Under direct irradiation, the photochemical reaction of singlet excited DBO goes via the C−N ring-opening transition state and subsequently a 4-fold crossing point to produce diazenyl biradical intermediates, which lose N_2 to form 1,4-cyclohexadiyl diradicals with almost no barriers. Due to efficient ISC, both singlet and triplet 1,4-cyclohexadiyl diradicals can be produced. (5) Under triplet-sensitized irradiation, the resulting triplet DBO decays via the C−N ring-opening transition state on the T_1 surface to produce N_2 and 1,4-cyclohexadiyl diradicals directly. In summary, this work presents a comprehensive and detailed picture of the photolysis mechanism of DBO, in excellent agreement with many experimental observations that have been reported on this species.

Acknowledgment. This work was supported by the National Basic Research Program (Grant No. 2004CB719901), the National Natural Science Foundation of China (Grant Nos. 20373022 and 20233020), and the Fok Ying Tong Education Foundation (Grant No. 91014). We owe special thanks to Prof. Thomas Bally (University of Fribourg, Switzerland) for his many useful suggestions, helpful discussions and careful editing of the original manuscript. We thank Virtual Laboratory of Computational Chemistry, Computer Network Information Center, Chinese Academy of Science for providing us with its computational resources.

Supporting Information Available: Calculated energies, Cartesian coordinates of all stationary points and crossing points, and the complete refs 32 and 35. This material is available free of charge via the Internet at http://pubs.acs.org.

JA050002P

(48) Caldwell, R. A.; Carlacci, L.; Doubleday, C. E., Jr.; Furlani, T. R.; King, H. F.; McIver, J. W., Jr. *J. Am. Chem. Soc.* **1988**, *110*, 6901.